

Small Demonstration Satellite-4 (SDS-4): Development, Flight Results, and Lessons Learned in JAXA's Microsatellite Project

Yosuke Nakamura, Kunitoshi Nishijo, Naomi Murakami, Kazutaka Kawashima, Yuuta Horikawa,
 Kazuhide Yamamoto, Takashi Ohtani, Yasuyuki Takhashi, and Koichi Inoue
 Japan Aerospace Exploration Agency (JAXA)
 2-1-1, Sengen, Tsukuba, Ibaraki, 305-8505, Japan; +81-50-3362-3475
 nakamura.yosuke@jaxa.jp

ABSTRACT

The Small Demonstration Satellite 4 (SDS-4) is the first zero momentum three-axis controlled 50kg class satellite from JAXA. It was launched on May 17, 2012 on H-IIA Launch Vehicle, and is now operating successfully. SDS-4 has four main demonstration missions: (1) Space-based automatic identification system experiment for tracking ships, (2) Flat-plate heat pipe on-orbit experiment, (3) Quartz crystal Microbalance for contamination environment monitoring, and (4) In-flight experiment of space materials using THERME, which is developed in the JAXA-CNES joint research program. The satellite has two deployable solar panels to the left and to the right, and two deployable AIS antennas in the front and in the back. In addition to the technology demonstration missions, SDS-4 has another important goal, namely to establish a 50 kg-class highly functional and precise three-axis controlled standard bus for future advanced missions. After a year of on-orbit experiments and evaluations, all missions are now deemed successful and excellent flight data has been obtained. We encountered several serious problems during operations. We investigated the reasons for those misbehaviors in a multi-step process using a methodical FTA approach, and managed finally to resolve all of the problems. This paper concludes with the lessons learned all of which contributed to the overall success of the SDS-4 project.

1. INTRODUCTION

JAXA has conducted a research and development program for small satellite systems and is now developing small, low-cost satellites to demonstrate advanced space technologies in orbit. These satellites are designed as piggyback payloads of the Japanese H-IIA launch vehicle with periodical launch opportunities. Our first small satellite, MicroLabSat, was launched on December 14, 2002 [1]. After this project, JAXA started a Technology Transfer Program for small and medium-sized enterprises (SMEs) in Japan to build a 50-kg class satellite "SOHLA-1". This satellite uses the components and bus technologies of MicroLabSat, and SME union engineers will acquire these basic technologies for new development and operation. In 2006, the Small Demonstration Satellite (SDS) program was initiated. This program has strategic meaning for JAXA's operational and science satellites, making it possible to discover the unexpected risks that might produce terrible results. It will open the door to adoption of next-generation space technologies. The missions were selected for the parts/components level, system/subsystem level, and mission-concept level based on the importance and urgency in JAXA's satellite-technology roadmap. SDS-1 is the first satellite in this program. It has three main missions components: (1) Multi-mode Integrated Transponder, (2) Space-wire

demonstration Module and super high sensitivity accelerometer for future gravitational wave observation; and (3) Advanced Micro processing In-orbit experiment equipment. The satellite was launched in January 2009. All missions were successful. Excellent results have been obtained including world's first achievement [2].

2. SDS-4 PROJECT

2.1. Satellite System Overview

SDS-4 is a 50-kg class satellite with three-axis Sun-oriented attitude control. Figure 1 shows in-orbit image of SDS-4. Table 1 presents main characteristics. The dimensions and weight are designed within the constraint of the H-IIA Launch Vehicle piggyback ride. Features of this satellite project include the following two objectives [3]:

- 1) To obtain 50 kg class SDS standard bus, achieving highly accurate three-axis zero-momentum attitude control performance required by future missions.
- 2) To demonstrate higher performance and smaller size satellite bus components such as an on-board computer, a high data rate S-band transponder, a power control unit, and ADCS components against past SDS satellites.

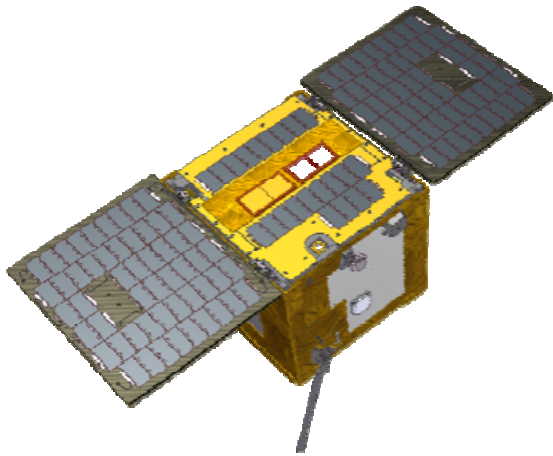


Figure 1: SDS-4

Table 1: Main characteristics

Weight	approx. 50 kg
Load Power	approx. 60 W
Size	500 × 500 × 450 mm (before deployment) 1400 × 500 × 450 mm (after deployment)
Attitude Control	three-axis Sun-oriented (Nominal) three-axis target pointing (Mission)
Communication	S-band Uplink: 4 kbps PCM-PSK/PM Downlink: 16 kbps PSM-PM (HK data) 1 Mbps QPSK (Mission data)
Orbit	SSO, altitude approx. 677 km

2.2. Missions

Besides these project objectives, SDS-4 has 4 different tech-demo missions which were selected from the proposals across the all JAXA's departments. Missions are selected from the viewpoints of their urgency and importance to future missions.

- 1) Space-based Automatic Identification System Experiment (SPAISE)[4]

The importance of maritime security has increased and JAXA has oriented AIS information for maritime security and safety in recent years. In Japan, maritime security and vessel traffic management are crucial because Japan is a maritime nation with a vast Exclusive Economic Zone (EEZ), and because many ships come from various countries for trade purposes. Traditional shore stations have collected AIS information from ships within a limited range and limited distance (typically about 74km). However, the Japanese EEZ is larger than the AIS area of coverage. Figure 2 shows the EEZ and AIS cover area in Japan.

SPAISE is proposed to resolve this problem with satellite based AIS-monitoring. SPAISE includes two missions; (1) engineering tests of the space-based

reception of AIS signals from ships, and (2) investigating the utility values of space-based AIS systems with joint researchers. The former is intended to solve problems related to the space-based reception of AIS signals from vessels, such as collisions of signals from ships due to the wider field of view from satellite, the Doppler shift due to the higher relative velocity of the satellite, and the Faraday rotation of polarization plane of AIS signals due to the ionosphere. The AIS receiver is constructed mainly from commercial products aim at low cost and quick development.

Figure 3 shows Space-based AIS concept of operations. Space-based AIS information is expected to contribute for maritime traffic monitoring, safety and security problems like piracy and criminal trespass. With an AIS transmitter equipped system, traveling ships can see where other vessels are and calculate their own course to avoid collisions. Constructing space-based infrastructure for AIS, including synthetic aperture radar satellites and ground management system, remains an ongoing task.



Figure 2: Japanese EEZ and ground-based AIS cover area

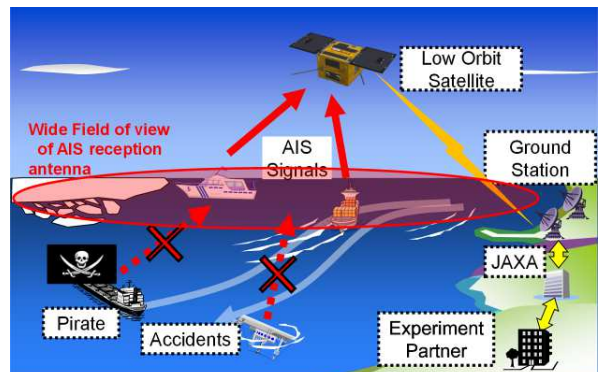


Figure 3: Space-based AIS operation concept

2) Flat-plate Heat Pipe (FHP) On-orbit Experiment (FOX):

FHP has a flat shape, which enables heat to be dissipated from the narrow clearance between the component and structure. The concept is shown in Figure 4. The FHP is a closed loop of smooth stainless steel tubing sandwiched between flat aluminum plates and charged with a working fluid inside. Figure 5 shows a picture of FHP flight model. The C-shape folded FHP is designed dedicated to SDS-4 to measure the performance within the limited space. The FOX mission demonstrates and confirms performance of the FHP with check valve under a Micro-G environment. FOX includes heaters at four different wattages to simulate components generating heat, and five temperature sensors are used to measure the effects of FHP.

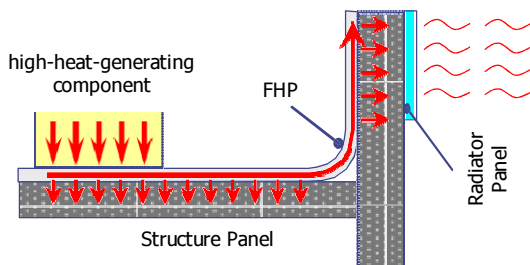


Figure 4: Concept of Flat plate Heat Pipe

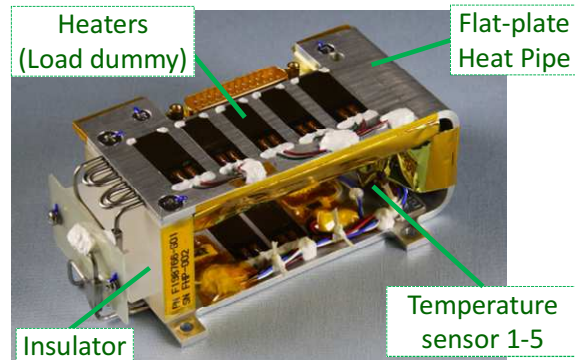


Figure 5: FOX flight model

3) Quartz Crystal Microbalance (QCM) contamination sensor

The mission is intended to demonstrate an economical, lightweight, compact and simple interface newly developed QCM, and measure the environmental contamination of spacecraft throughout the whole life cycle; from assembly, integration, and testing to in-orbit operation. Figure 6 shows a flight model of QCM and an inner sensor, which will be used to measure chemical and electric thruster exhaust plumes or the atomic oxygen (AO) environment in future science missions.

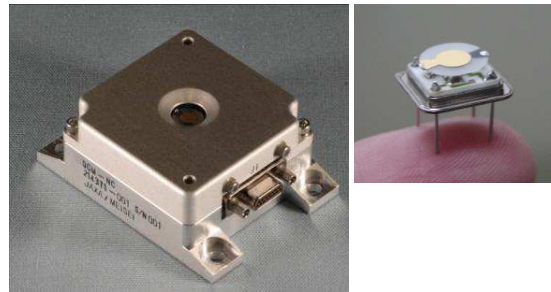


Figure 6: Quartz Crystal Microbalance (QCM) contamination sensor

4) In-flight experiments related to Space materials using THERME (IST)[5]

The IST mission measures solar absorptance and the degradation characteristics of the new thermal control materials. This mission is conducted as a JAXA-CNES joint research program. CNES has developed very simple and inexpensive experimental equipments known as "THERME". THERME consists of sample materials, MLI and temperature sensors. The temperature reached under the same incidence condition of sunlight depends on the change of α_s , which can be calculated from measured temperature, assuming that the infrared emittance (ε_{IR}) of a sample remains stable in terms of BOL value. Figure 7 shows an overview of THERME. The JAXA samples are thermal control films, i.e., aluminized AO-tolerant polyimide film "BSF-30" with/without UV protective coating.



Figure 7: THERME flight model (JAXA sample)

2.3. Project Team

SDS satellites are designed, hand-constructed, tested, and operated by JAXA's young engineers. This program is also positioned as a part of a capacity-building program. SDS program offers an opportunity to design, fabricate, integrate, and test satellites, and manage the whole process of the projects to young engineers. It serves as an effective learning tool for building engineers' spacecraft development capacity. The number of JAXA team members in SDS-4 project is around fifteen; half of them are young engineers in their 20's.

3. TECHNICAL CHALLENGES OF SDS-4

3.1. System Architecture

The system block diagram of the SDS-4 is shown in Figure 8. The architecture of SDS-4 is designed to be simple, with single non-redundant bus components. Adoption of commercial off-the-shelf (COTS) parts is allowed, if necessary, with adequate radiation testing. Critical bus components such as a power control unit, transponder, and components for attitude determination are connected to extended module 1 of on-board computer. This enables to minimize power consumption in low load mode by switching off the extended module 2 and other non essential components.

3.2. Three-axis Zero-momentum Attitude Control

The attitude determination is based on Extended Kalman-filter (EKF) estimation using a star tracker (STT), a digital sun sensor (DSS), a magnetic sensor (MAGS) and a newly developed high accuracy three axis MEMS gyro[6],[7]. 5 coarse sun sensors are used for detection of the sun. In most of the time, gyro-stellar attitude determination is used, but since SDS-4 has only one STT, there is a certain period of time that sunlight or albedo of the Earth comes into the field of view of the STT. During that period, the sun and magnetic field vectors in the body frame are measured using a digital

sun sensor and MAGS, the two pairs of vectors are used to calculate the inertial-to-body attitude quaternion using the QUEST (QUaternion ESTimator) algorithm.

During normal operations, the generation of control torque is ensured by three reaction wheels (RW). Their storage capacity is 0.42 Nms and their maximum torque capability is 10 mNm. Momentum dumping is ensured by a three-axis MAGS and magnetic torquer rods (MTQ). These MAGSs and actuators are also used during the initial attitude acquisition operations, to reduce the body angular rates induced by the launcher at separation. Zero-momentum control technique enables agile attitude maneuvers.

The attitude determination and control subsystem (ADCS) can be operated in the 5 operational modes shown in Figure 9. Transition between any of them is possible and can be commanded either by the ground station or autonomously, by the on-board mode manager. The Rate Damping Mode (RDM) and Sun Acquisition Mode (SAM) are the most critical enabling the System Safe mode, while the Sun Pointing Mode (SPM) and Earth Pointing Mode (EPM) are required to provide nominal mission operations. The suffix -C and -F in SPM and EPM indicate “Coarse” attitude determination using a sun sensor and a MAGS, and “Fine” attitude determination using a STT, respectively.

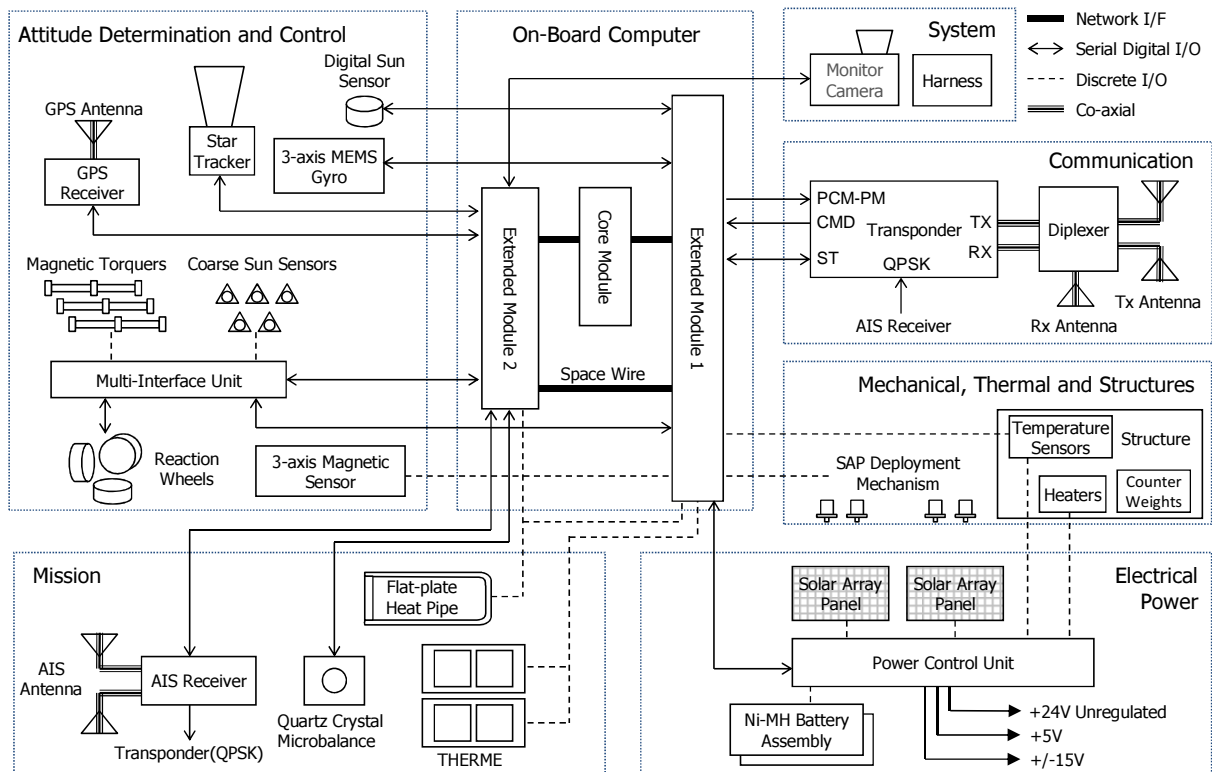


Figure 8: System block diagram of SDS-4

The Attitude Control Flight Software (ACFS) is installed on the on-board computer. Although SDS-4 has no redundant hardware, carefully designed fault detection, isolation and reconfiguration (FDIR) adds functional redundancy on ADCS. In case of a failure in ADCS, FDIR function immediately detects it and changes ADCS configuration and control mode. A newly developed general-purpose on-board computer enabled to perform elaborate calculations.

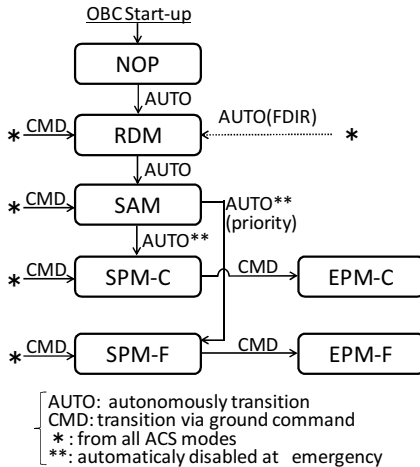


Figure 9: ADCS Modes

3.3. High Density Component Layout

Satellite design of SDS-4 is based on heritages of SDS-1. But SDS-1 was 100kg satellite, so that we had to redesign components to miniaturize, and packed into the small structure. It was also a big challenge to supply enough room for mission components while ensuring structure and thermal design and accessibility. Figure 10 shows inner layout of SDS-4. The satellite structure is divided into two areas. The most accessed components, the power control unit and the on-board computer, are arranged on the front and back access panels.

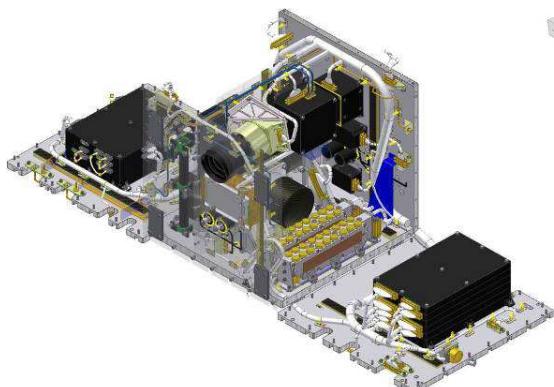


Figure 10: Inner layout (upper panel and access panels opened)

In order to stabilize inner temperature, we applied a heat shield on the upper sun pointing panel shown in Figure 11. The heat shield is mounted through insulators. The surface of the heat shield is finished very smooth to obtain low ϵ , which enables low heat transfer between the heat shield and main structure.

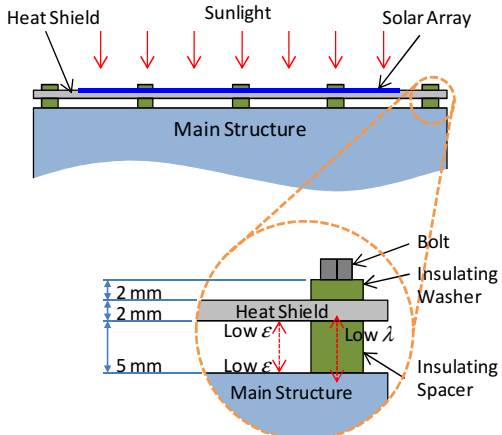


Figure 11: Heat shield for thermal stability

4. DEVELOPMENT OF SDS-4

4.1. Overview

The schedule of SDS-4 project is shown in Figure 12. Conceptual study of SDS-4 was done in 2009 and the project began in January 2010. After development and testings of breadboard models (BBM), engineering models (EM) and satellite thermal and structural model, system design review, which corresponds to merged version of Preliminary Design Review (PDR) and Critical Design Review (CDR), was conducted and flight model production and testing phase started in November 2010.

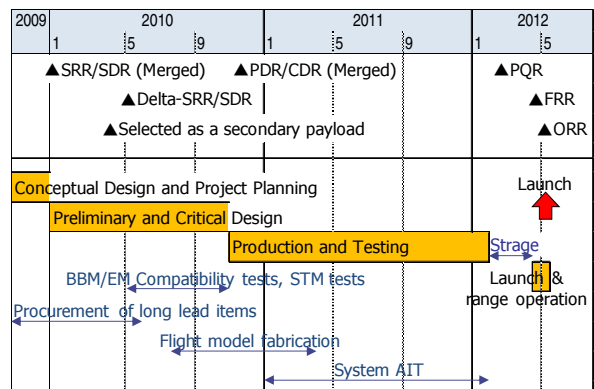


Figure 12: SDS-4 development schedule

During the System Assembly, Integration and Testing (AIT) phase, the big earthquake hit the eastern part of Japan. Tsukuba Space Center, where is north east of Tokyo and our laboratory is located, shook badly during the earthquake. System AIT finished in February 2012, and the satellite was carried to launch site, Tanegashima Space Center, for range operation in April 2012.

Especially, in this chapter, we focus on the aftermaths of the earthquake, system real sky test and electromagnetic compatibility (EMC) test.

4.2. Aftermaths of the big earthquake in eastern part of Japan

We were conducting system integration when the big earthquake hit eastern part of Japan in March 11, 2011. Although our project office was damaged severely as shown in Figure 13, there was no damage on flight hardware and no project team members were injured. We conducted health check and trend data evaluation of the satellite as well as analytical verification.

Due to the earthquake, satellite test buildings in JAXA Tsukuba Space Center were damaged, electrical power was insufficient for the first few months all over the nation, and Japanese industries had stagnated. We could finally get over these difficulties and the launch schedule delay was only half a year.



Figure 13: Collapsed project office after 3.11

4.3. System EMC test for SPAISE mission

We encountered various difficulties in SPAISE integrated tests. The SPAISE mission requirement on the system noise of the satellite was so strict that we spent a total of around 2 months on EMC test in the radio wave test building in order to reduce system noise to around 162 MHz which is the frequency used for AIS signals.

The noise frequency was emitted from the satellite system and the EMC testing setup itself. In particular, constructing the test system takes considerable time. We took off a solar array simulator which makes large noise, and instead, connected external batteries to

supply power to the satellite. The umbilical line from the SDS-4 was also removed physically to avoid noise emission from the cable. Thus the satellite was operated completely wireless configuration. A multi-pass problem arose from the satellite mounting support structure, so we also removed it from the SDS-4 and instead, we suspended the SDS-4 on a crane and setting it on a mounting made of polystyrene foam. Figure 14 shows the configuration of the SPAISE integrated performance test.

As a countermeasure to the satellite system noise, we attached an additional electro-magnetic shield fabric, which is weaved using metal fibers and nylon fibers, to the on-board computer, as shown in Figure 15, the power control unit, AIS receiver, and part of the system harness line. Aluminum tape was also attached between the structure panels to enhance the conductivity between structure panels and to reduce noise leakage. The switching noise produced from a regulator in the power control unit was also the big source of system noise. There were two types of regulator's duty control mode, a hardware based control and a software based control. After the several tests, we found that the hardware based regulator control was making bigger noise. Thus, we decided to conduct SPAISE mission operation in the software based regulator control mode.



Figure 14: System EMC test configuration

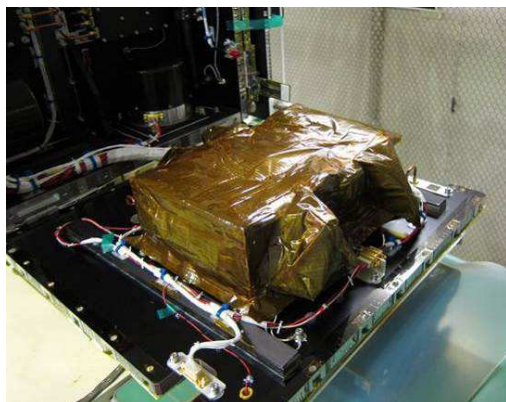


Figure 15: Added electro-magnetic shield fabric to cover the on-board computer

4.4. System Real Sky Test

The real sky tests using the SDS-4 PFM are very unique taking advantage of micro satellites. The SDS-4 system flight model was located outdoors and implemented dynamic attitude determination using a STT, a gyro, a DSS, and a MAGS. Through these tests, we confirmed the end-to-end function of the attitude determination and control, including verification of its performance and polarity of components. The relatively small satellite allowed such an adventurous test using real sky.

Figure 16 shows attitude determination test using a STT and a gyro at night. The satellite was turned over 90 degrees and a solar array panel (SAP) was deployed to make a STT mounted on the side panel to see the sky. Figure 17 is also an attitude determination test using a DSS, a MAGS and a gyro under the day light. Earth's magnetic field was calibrated using external magnetic sensor. The satellite was protected from outside contamination by a clear plastic container.

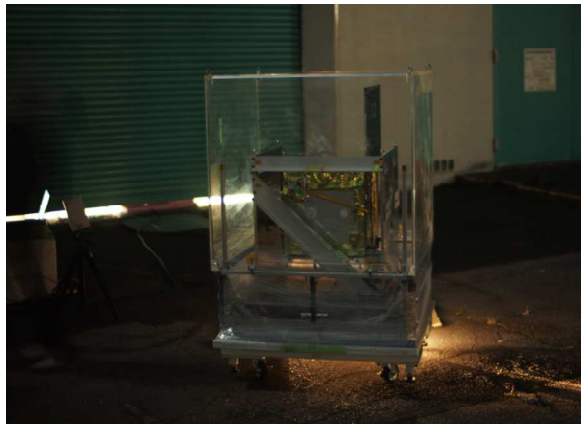


Figure 16: Real sky test, or night sky test, for a STT and a gyro



Figure 17: Real sky test under day light for a sun sensor, a MAGS and a gyro

5. FLIGHT RESULTS

5.1. Overview

SDS-4 was launched on May 18, 2012 on an H-IIA Launch Vehicle with GCOM-W1 (Global Change Observation Mission 1st - Water), KOMPSAT-3 (Korean Multi-Purpose Satellite-3) and another small satellite. (Figure 18) Operation of SDS-4 is conducted using JAXA's ground stations located at all over the world, and Kongsberg Satellite Services (KSAT) located at Norway.

Operation phases are divided in four, and Figure 19 summarizes them. Currently, the SDS-4 operation is in the post-mission phase.



Figure 18: Launch of SDS-4

May 18, 2012	✓ Launch
2 days	Early Operation Phase
	✓ Power on, separation, rate dumping, SAP deployment ✓ Sun acquisition ✓ Establishment of communication, and power ✓ Initial orbit determination
May 20, 2012	✓ Establishment of inertially fixed 3-axis control
1 Month	Commissioning Phase
	✓ AIS antenna deployment ✓ All components checkout ✓ Orbit determination by 2-way Doppler ✓ Commissioning Phase Review
June 19, 2012	✓ Mission operation to achieve full successes ✓ Evaluation of trend data ✓ Post-Nominal Operation Review
5 Months	Nominal Operation Phase
	✓ Mission operation to achieve extra successes ✓ Additional experiments ✓ Evaluation of trend data ✓ Outreach activities utilizing satellite operations
Nov. 17, 2012	Post-mission Phase

Figure 19: Operation schedule

5.2. Early operation and Commissioning Phase

The 1st telemetry data from the SDS-4 was obtained via the KSAT ground station and the satellite health status was confirmed. Two SAPs were deployed by the auto sequence, the result of which was confirmed by the picture taken by the monitoring camera (MCMR) shown in Figure 20. The left side object in the picture is the SAP.



Figure 20: Picture taken by MCMR

Figure 21 shows anomaly in received signal strength indication (RSSI) of SDS-4 in orbit. Blue dots indicate RSSI increase during operation. Strength of signals differs according to the ground station used, JAXA or KAT, the attitude, antenna pattern, and relative position of the SDS-4 in orbit, and the maximum strength in each operation is around -80~-60 dBm. But as shown by red dots in the plot, RSSI increased up to -87dBm during the periods when there is no uplink carrier wave from ground. This phenomenon caused a serious problem in satellite operation, because the unknown noise suppressed the uplink signal and this come out as bit errors in the commands. We investigated the reason thoroughly, but it is still unknown. This noise disappeared just after two days from launch.

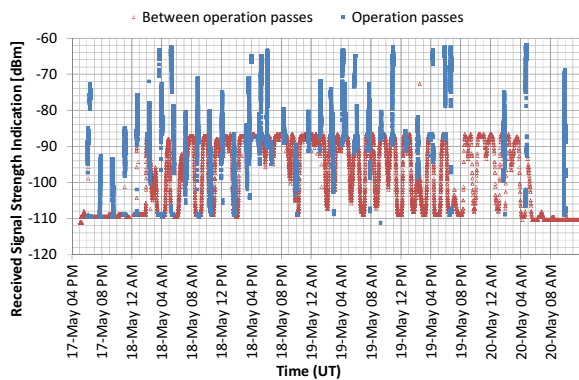


Figure 21: RSSI anomaly in the early operation phase

After the early operation phase, the Commissioning phase lasted for one month. ADCS mode was changed from SPM to SPM, all components checkout, including mission components and SPAISE antenna deployment, were conducted, and all were successfully completed.

5.3. Nominal operation and Post-mission Phase

The nominal operation phase lasted five months. During this phase, mission operations were conducted and achieved full success. We evaluated the performance of bus components in orbit, such as the bit inversion in the memories of the on-board computer, generation power of solar arrays, the capacity degradation of Ni-MH batteries, transmission power of transponder, loss torque of WHLs and so on. The trend graph of the battery voltage at the end of eclipse is shown in Figure 22, where red dots are in orbit data and blue dots are data obtained in cycle test on ground. The voltage changes depending on the depth of discharge, but overall trend fits well to the ground test data. The lower limit of the voltage, that is to say the end of life, is 1.1V, so it seems that the battery can last at least a few more years.

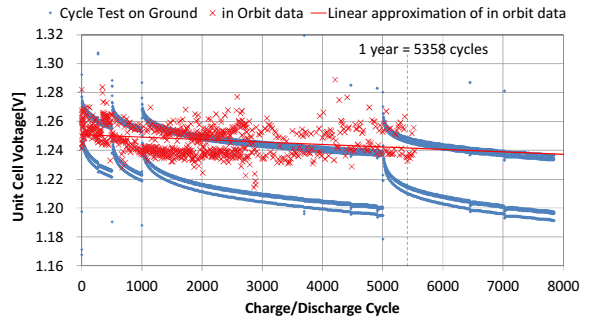


Figure 22: Ni-MH battery trend data

The following two plots in Figure 24 show controller input angle in ACFS. The upper figure shows results obtained over a period of 10 orbits (16.6 hours) while the bottom shows specific 5 minutes profile. The controller input angle represents the pointing error angle in the Sun frame and exclude the 1.63deg (3σ) attitude estimation errors of the EKF caused by gyro noise and STT noise modeling errors. It is possible to observe how the regular peak corresponds to the attitude propagation errors in the plots. This behavior is normal since some star sensor measurements are invalid during the earth exclusion and sun exclusion light.

The mean and standard deviation values of attitude error are summarized in Table 2. The crossover frequency is designed as Y>Z>X, while the residual error of 3σ shows the correct frequency order[8].

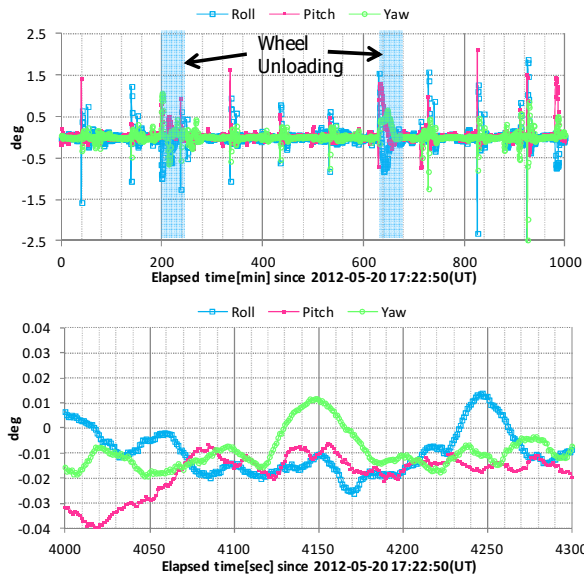


Figure 23: Controller input angle (upper: 16.6 hours, bottom: 5 minutes)

Table 2: SPM/EPM Controller Performance

Satellite Body Axis	Mean Error [deg]	3 σ [deg]	Peak-to-Peak over 5min [deg]
X	-0.01	0.538	0.040
Y	0.017	0.455	0.035
Z	0.144	0.401	0.030

Figure 24 shows the wheel speed, while the wheels running from 350 to 750 RPM and momentum unloading activated every 3.9 hours. The estimated disturbance torque and magnetic torquers' performances are equal to the design values.

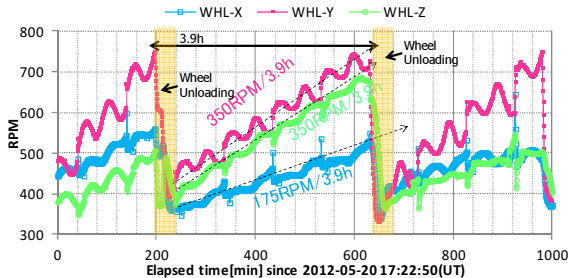


Figure 24: Wheel angular speed profile

5.4. Post-mission Phase

To enhance the mission and conduct new experiments, a post-mission phase started in November 2012, and remains ongoing. For example, SPAISE experiments with attitude control are conducted for extra success,

after confirming feasibility from a view point of each subsystem before the operation.

As a labor-saving operation, the preparation time and persons involved in the SDS-4 operation can be reduced by improving the operating support tools during the post-mission phase. Automated operation software will be also implemented for sequence fixed operations such as housekeeping and SPAISE mission operations.

5.5. Result of Mission Operations

1) SPISE

The on-board AIS receiver successfully received AIS signals and confirmed the function and performance in orbit. The receiver received signals from up to 336 ships over a minute, with 5000 km^2 covered by a single AIS antenna. As previously assumed, collisions among messages occurred in ships in congested areas of China and Japan, which caused the reception rate to decline. Currently we are conducting experiments to enhance the reception rate of AIS signals in congested areas by changing the satellite attitude. Figure 25 shows the position plotting of the AIS signal in Japanese coastal waters for 68 days.

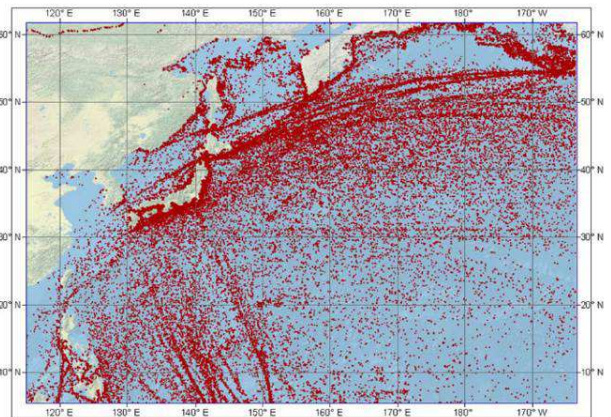


Figure 25: Position Plotting of the AIS signal in Japanese coastal waters

2) FOX

A stable running performance of FHP with check valve was confirmed for the first time in the world. By matching amount of heat transport and thermal conductivity of orbit data with analytical result and ground test results, the function and performance, are confirmed. Figure 26 shows that the temperature of cooling part of FHP follows the heating part within 5 degrees, which means the FHP is transferring heats stably through the one cycle of orbit.

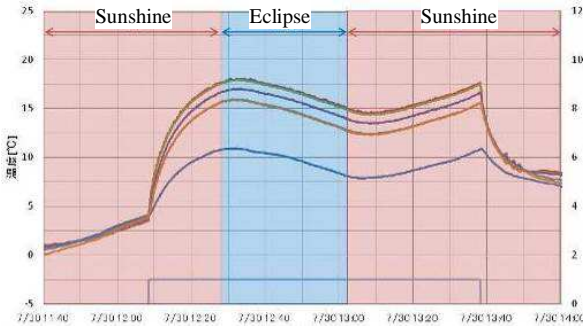


Figure 26: Effect of the flat-plate heat pipe

3) QCM

Figure 27 shows frequency trend of QCM from ground test to in orbit operation. The frequency decreases slowly on the ground and rises sharply just after the launch of SDS-4. That means contaminants deposits on the membrane during the ground test, and the mass on the membrane got bigger, thus frequency decreases. This trend is followed by removal contaminants due to the atomic oxygen on orbit, decrement in the mass on the membrane, and increment on its frequency. There is no trend toward deposition of contaminants.

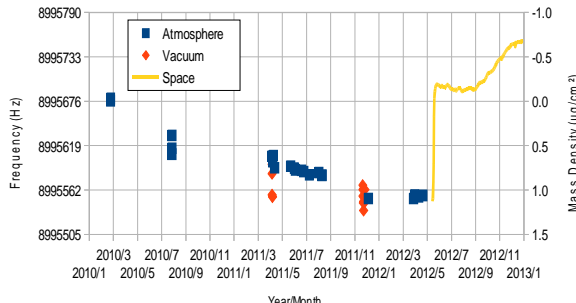


Figure 27: Variation of attached contaminants mass on QCM from ground test to orbit

4) IST

Solar absorptance coefficient (α_s) is expressed in following equation;

$$\alpha_s = \varepsilon_{IR} \sigma T^4 / C_s \cos \theta$$

where A is surface area of a sample material, C_s is the solar constant, θ is solar incident angle, ε_{IR} is infrared emissivity of a sample material, σ is Boltzmann constant, and T is temperature of a sample. Supposing that ε_{IR} does not change in the mission period, α_s can be obtained by measuring the temperature.

Figure 28 shows degradation of solar absorptance coefficient of materials. The effect of UV-shielded coating was verified based on the variation in solar absorptance coefficient. The variation in α_s is

considered due to ultraviolet degradation by comparing with the ground test result.

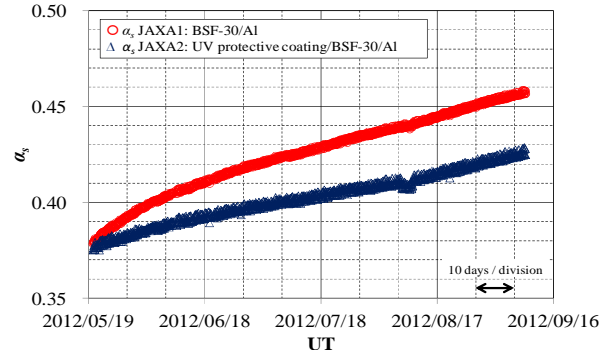


Figure 28: Degradation of solar absorptance coefficient

6. LESSONS LEARNED

6.1. Design and Analysis

1) Too strict FDIR error threshold settings

In the early operation phase, ACFS had detected several FDIR events, and the ADCS mode was forced to change in the safe rate damping mode. But after the investigations, we found that there were no malfunctioning in the system, and they were just because of the too strict settings in the error limits of FDIR function. Especially in constant value error detection, which is designed considering a failure in AD converters, AD converted value are more stable than expected from ground test. So as a matter of fact, random noise in space was smaller than it was on ground, but since the constant error threshold values were determined using ground test data, FDIR function judged very stable constant values on orbit as an error.

2) Availability of STT

STT availability is the key factor determining the performance of attitude determination. But there has been a significant difference between actual in-orbit and predicted availabilities.

Figure 29 shows the typical trend of STT availability which was predicted (on the left) and that actually obtained in orbit (on the right). The orange and pink dots indicate the regions where valid STT measurement is obtained. Unlike the preflight understanding, STT can provide attitude quaternions for almost all eclipse regions. In addition, it becomes available before entering the eclipse period. This situation is preferable, and suggests that STT can continue measurements when the Earth partially masks its field of view, and that the Earth exclusion angle of STT may be narrower.

Conversely, STT is regularly unavailable for more than half the period of sunlight, which is likely attributable to its inappropriate layout. It seems the sunlight reflected from the Earth's surface is re-reflected by the back surface of the satellite's solar panel and enters the Earth exclusion angle, resulting in the unavailability of STT during periods of sunlight. Figure 30 shows the schematics of the STT layout, with the edge of the Earth exclusion angle crossing the solar panel. Picture of Figure 31 was taken by the on-board monitor camera attached to the opposite side of STT, which indicates that the back surface of the solar panel is lightened by the albedo of the Earth. It is noted that STT sometimes provides valid but inaccurate quaternion randomly during such regions, which increases the error rate for attitude determination.

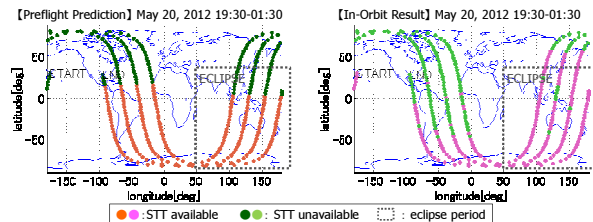


Figure 29: STT availability comparison

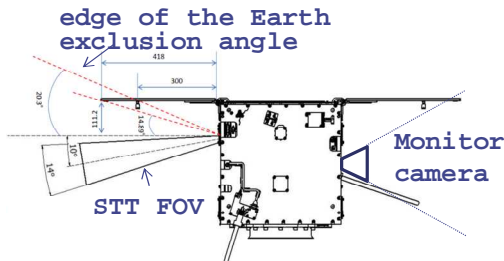


Figure 30: Layout and FOV of the STT



Figure 31: Back surface of the solar panel is lightened by the albedo light of the Earth

3) Unexpected attitude loss due to the EKF reset

SDS-4 ACS has a function to reset the EKF attitude estimation shown in Figure 32. Here, ‘reset’ means initializing the predicted (a priori) estimate covariance matrix P into a big number. When the difference between predicted and measured quaternions, Δy , exceeds the predetermined threshold, P is automatically

initialized. This function is added to avoid EKF divergence in the event of any anomaly. However, the EKF reset occurred far more frequently than expected, sometimes resulting in severe situations such as attitude loss.

$$\begin{aligned} \Delta y(t) &= \mathbf{q}_{ref}(t) \oplus (-\mathbf{q}_{meas}(t)) \\ \begin{bmatrix} \Delta \hat{\mathbf{q}}_v(t) \\ \Delta \hat{\mathbf{b}}(t) \end{bmatrix} &= \mathbf{K}(t) \Delta y(t) \\ \rightarrow \begin{bmatrix} \Delta \hat{b}_x(t) \\ \Delta \hat{b}_y(t) \\ \Delta \hat{b}_z(t) \end{bmatrix} &= \begin{bmatrix} K_{41} & K_{42} & K_{43} \\ K_{51} & K_{52} & K_{53} \\ K_{61} & K_{62} & K_{63} \end{bmatrix}(t) \cdot \begin{bmatrix} \Delta y_1(t) \\ \Delta y_2(t) \\ \Delta y_3(t) \end{bmatrix} \\ \hat{\mathbf{b}}(t) &= \bar{\mathbf{b}}(t) + \Delta \hat{\mathbf{b}}(t) \end{aligned}$$

Figure 32: Kalman gain and rate bias estimation

This was attributable to the following four factors: (1) anomalous behavior of STT, (2) inappropriate threshold setting, (3) larger error in a MAGS measurement, and (4) inappropriate initialized value of matrix P. As mentioned above, STT measurement becomes unavailable for some time during periods of sunlight. The problem is that, shortly before it becomes completely unavailable, STT randomly provides quaternions which contain significant errors. When such errors exceed the threshold level, the EKF reset occurs. In addition, since the error in MAGS measurement was larger in orbit before calibration than that measured in the ground test, the calculated attitude via the QUEST method also had significant errors, which sometimes exceed the threshold. A severe situation occurs when such error output persists after the EKF reset, resulting in a significant error in estimating gyro rate bias. The Kalman gain K determines how much Δy is assumed for the updated estimation error Δb . If anomalous measurement continues and Δy remains large after the EKF reset, the estimated rate bias b becomes much larger than its true state. If measurement update stops at this point, attitude propagation must start with such significant bias errors, which eventually result in a loss of satellite attitude.

After this event, the threshold for the EKF reset was updated with a sufficient margin, considering the anomalous STT output and the measurement error of a MAGS. Additionally, in preparation for further anomaly in STT, which possibly causes such situations again, we examined the threshold settings for the QUEST measurement with a number of experimental operations and concluded that no restriction is preferable. This result also contributed to the improvement in the attitude determination accuracy. Fundamental solution is to initialize the matrix P with moderate value.

4) Sunlight refraction effect on gyro rate bias estimation

Since a DSS is attached to the same surface as the solar panels, the sun angle detected by the DSS ought to be zero when the three-axis control is successfully conducted. However, as shown in Figure 33, the sun angle data always indicates a steep increase, reaching about 1.5 degrees when the satellite is entering or exiting an eclipse. This can be explained by the refraction of sunlight in the Earth's atmosphere. The in Figure 34 shows a conceptual diagram of the sunlight refraction effect.

Since the measurement update is conducted with STT during those periods, the attitude determination is unaffected by sunlight refraction and the satellite is controlled inertially-fixed. However, for the QUEST attitude determination, the sunlight refraction applied a certain error, since the QUEST method uses the sun vector detected by DSS. According to the in-orbit experiment in which the QUEST attitude is used to update measurement during those periods, the generated errors in the EKF estimation of satellite's attitude and gyro bias rate reached about 0.06 deg and 0.001 degree/s, respectively. To reduce such errors, tuning of the measurement noise covariance and inhibiting the use of the QUEST attitude during those periods were found to be effective through experimental operations.

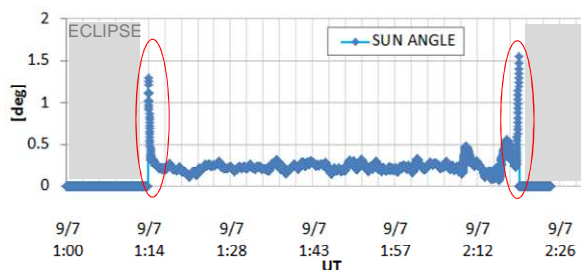


Figure 33: Steep increase of the sun angle

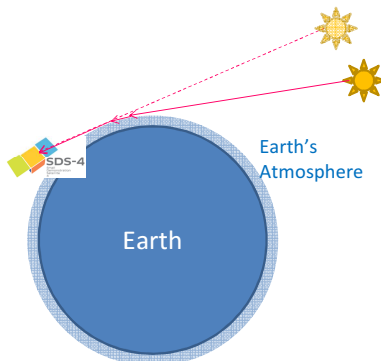


Figure 34: Sunlight Refraction Effect

5) Oscillatory response in the satellite's angular rate

Although the following event was found to have no direct relationship with the attitude determination, we introduce it as an interesting case: Small oscillatory responses in the satellite angular rate were occasionally observed in orbit. The rotation speed data of RWs also showed the same responses during these periods. Figure 35 indicates the angular rate of the satellite and the rotation speed of RW under such events.

The responses appeared and faded without any particular trigger, and occurred even before three-axis control was started. After a month of investigation, it was found that these responses were likely to be caused by the aliasing effect between the ACS controller sampling and the nearly sinusoidal noise on the rotation speed telemetry of RWs. The RW of SDS-4 has a speed control loop and it is driven at a speed command from ACS. The ground test results showed that the rotation speed telemetry of RW has nearly sinusoidal noise whose frequency $f_{RW\text{noise}}$ ranges from 0 to 2.5 Hz, depending on its rotation speed, as shown in Figure 36. When ACS samples the telemetry data at the ACS control frequency f_{ACS} of 1Hz, the observed RW speed fluctuates at a frequency of

$$f = f_{ACS} - f_{RW\text{noise}}$$

due to an aliasing effect. If it reaches to the ACS control bandwidth of $\omega_c = 0.006 - 0.008$ Hz, that is to say, the noise frequency $f_{RW\text{noise}}$ comes close to 1 or 2 Hz, ACS controller responses to this fluctuation and the satellite begins to show the oscillatory response. Figure 35 shows that the oscillation occurs when the RW speed is about 60, 120 and -240 rpm, in which the frequency of the sinusoidal noise is about 1, 2 and 1 Hz, respectively. It is noted that the amplitudes of these responses are negligible and such responses are certain to fade according to the change in the RW speed.

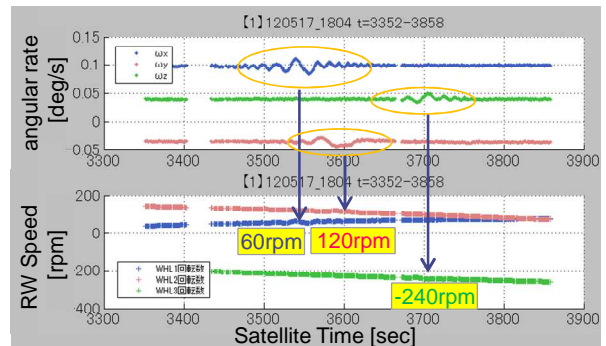


Figure 35: Oscillatory Response in Satellite's angular rate and RW Rotation Speed

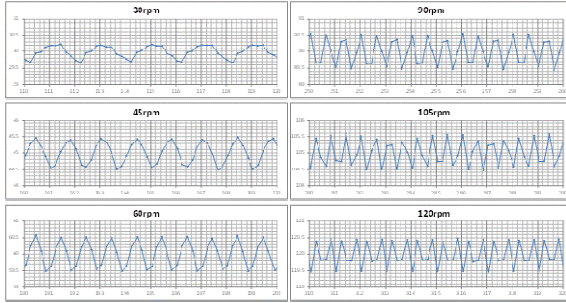


Figure 36: Sinusoidal Noise on the RW Rotation Speed

6.2. Development and Management

1) Reduction of development phase segmentation

In the project planning phase, we decided to merge SRR and SDR, and PDR and CDR. Usually in small satellite projects, schedule is the most strict limitation. Segmentalized project phases will come up with unnecessary schedule margins. On the other hands, merging phases may encompass risks such as schedule delay due to development troubles. In order to handle these risks, a project manager has to prepare a project margin.

2) System level End-to-End testing policy:

Conduct system level End-to-End system tests to the extent possible. This policy is very effective for relatively small space crafts.

At the system EMC test, first mission requirement from SPAISE mission was defined in system noise level, which was very small that the value was far below the measurement limit of a oscilloscope. As the EMC test progressed, we came to understand that defining requirement with intermediate value between mission component and satellite bus is not important. And finally, the requirement was redefined with bit error rate on AIS signal. This change eliminated unnecessary interface margins and we could satisfy required performance of AIS receiver.

System real sky tests were one of most exciting and challenging End-to-End tests in AIT phase. Although we could not find any bugs on the software, we could have very strong confidence on mission success through the test.

Furthermore, in the final system operation simulation test, we could find the polarity definition mistakes of reaction wheels just 4 days before shipment to the launch site. It was found by staring direction of rotation of a rotor from the hole on the cover.

3) AIS signal generator for SPAISE ground testing

When you deal with new technologies, in order to concentrate on the new things, you had better rely on a proven simulation and verification test environment.

It was the first time for JAXA to develop a space-based AIS receiver. AIS signal generator to test the receiver was also developed in parallel with the receiver. But as a part of risk management, we bought another AIS signal generator which can simulate collision and delays on the AIS signal received in orbit. The signal generator had many heritages in the past space-based AIS projects in foreign countries.

As a result, we had many troubles in the hardware of the AIS receiver, and debugging of originally developed signal generator was postponed. Using the proven signal generator, we could find a bug in the synchronization of AIS signals, which could not be found by the signal generator developed by JAXA. It was also useful in the total performance evaluation of the AIS receiver.

4) Squawk list

Squawk list is a list where any tiny phenomena noticed during tests, such as a very small spike noise found on an oscilloscope or even in the situation that is something strange but the reason is unknown, are written down. Figure 37 shows accumulated number of squawks during system AIT. The numbers of squawks were finally up to 500. This list greatly helped us finding mistakes in design and manufacturing of the satellite, and bugs in the on-board software.

If someone noticed a problem, we do not blame on the mistake, but instead, we think positively that we are approaching success. This custom motivated project team members to find more squawks during system tests. Since there are too many squawks, we put weight on each squawk, and addressed in order. These efforts contributed to the overall success of the SDS-4 project.

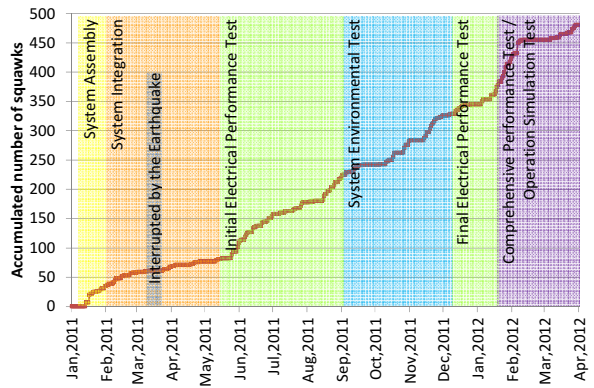


Figure 37: Accumulated number of squawks

6.3. Operations

- 1) Check the telemetry data thoroughly even though it looks good

In the 1st Acquisition of Signal (AOS) pass of SDS-4 just after the launch, the health status of the satellite looked very good except one telemetry data that seems not so important. Everyone rejoiced and started celebrating the successful launch. The 2nd AOS was just 5 minutes after the 1st AOS, and it was also successful and the attitude was in Sun Acquisition Mode. But in the 3rd AOS, the situation changed badly. The satellite ACFS detected a FDIR event, and the attitude was in Rate Damping Mode, that means the solar panels not pointing toward the Sun. We could recover the attitude in the 4th AOS. After the investigation, we found that the sign of malfunctioning had been seen already from the 1st AOS. It is important to check the telemetry if there is even the slightest grounds for doubt.

- 2) Prevention of operational mistakes using an automatic operation procedure generation tool

Since SPAISE was the first AIS mission for JAXA, the hardware development of the component was mainly focused. Therefore, to be flexible in mission operations on orbit, relatively primitive commands are arranged. To conduct complicated operations, these primitive commands have to be combined, and that made the number of commands increased. Moreover, it was after launch that we could make detailed operation plan, because the mission operation required maximum actual satellite resources. As a results, preparing mission operations took considerable efforts because of the complicated operation procedures, and produced human errors. It also took considerable time to confirm the procedures. To solve this problem, we introduced an automatic procedure generation tool for SPAISE, which automatically compiles an experiment plan to an operation procedure. To facilitate and streamline preparation, and to reduce human errors, we found it important to relegate the analog work to software, which saves labor as well.

7. CONCLUSION

As presented in this paper, we described an overview of the SDS-4 spacecraft, and its flight results. The satellite was launched on 18 May, 2012. The SDS-4 mission achieved full success and the SDS-4 continues to collect valuable mission data, remaining in full working order. These mission results were applied in the JAXA's future operational satellites and science satellites.

In addition, the performance of 50 kg class SDS standard satellite bus was verified in orbit. It achieved highly accurate three-axis zero-momentum attitude control. Small satellite bus components such as an on-board computer, a high data rate S-band transponder, a power control unit, and ADCS components were also demonstrated in orbit. These standard bus technologies are deployed among Japanese industries and academia to enhance capability of small satellite missions. Moreover, the lessons learned will be applied to the next small satellite project in JAXA.

References

1. T. Nakamura, A. Noda, H. Hashimoto, S. Kimura, S. Nishida and S. Nakasuka, "Micro-Labsat", IAC-03-IAA.11.1.08, Proceedings of the 54th International Astronautical Congress, Bremen, 2003.
2. Y. Nakamura, K. Kawashima, K. Yamamoto, K. Shinoda, H. Kawara, K. Hirako, and H. Hashimoto, "Flight Result of SDS-1", Proc. of the 4S Symp., Small Satellites, Systems and Services, Madeira, Portugal, 2010.
3. T. Ohtani, Y. Nakamura, Y. Takahashi, K. Inoue, and K. Hirako, "FIRST FLIGHT RESULT OF JAPANESE TECHNOLOGY DEMONSTRATION MISSION SDS-4", IAC-12-B4.6A.2, Proceedings of the 63rd International Astronautical Congress, Naples, Italy 2012
4. M. Abe, "The Concept of Space-based Automatic Identification System Experiment (SPAISE)," Proceedings of the 28th ISTS (International Symposium on Space Technology and Science), Okinawa, Japan, June 5-12, 2011, paper: 2011-j-18
5. E. Miyazaki, S. Remaury, Y. Nakamura, Y. Kimoto, K. Fujihira, P. Nabarra, and S. d'Escrivan, "'IST': Collaborative Flight Experimental Mission between CNES and JAXA on JAXA Satellite SDS-4 for the Evaluation of Thermal Control Materials in LEO", 12th International Symposium on Materials in the Space Environment, Noordwijk, Netherlands, 2012
6. N. Murakami, Y. Nakajima, T. Ohtani, Y. Nakamura, K. Inoue, K. Hirako, "First Flight Result of Attitude Determination for 50 kg class Micro Satellite SDS-4", 22nd International Symposium on Space Flight Dynamics, 2011.
7. Y. Nakajima, Y. Nakamura, H. Kawara, N. Murakami, T. Ohtani, K. Inoue, K. Hirako,

- “Development of High Accuracy MEMS Rate Sensor for Small Satellites,” Proceedings of IAC 2011 (62nd International Astronautical Congress), Cape Town, South Africa, Oct. 3-7, 2011, paper: IAC-11-B4.6A.11
8. Y. Nakajima, N. Murakami, T. Ohtani, Y. Nakamura, K. Inoue, K. Hirako, “SDS-4 Attitude Control System: First Flight Results of Attitude Control Response”, IAC-12.C1.9.3, Proceedings of the 63rd International Astronautical Congress, Napoli, Italy, 2012.